HHS Public Access

Author manuscript

Biosens Bioelectron. Author manuscript; available in PMC 2018 January 10.

Published in final edited form as:

Biosens Bioelectron. 2017 December 15; 98: 305–309. doi:10.1016/j.bios.2017.07.014.

Portable amperometric immunosensor for histamine detection using Prussian blue-chitosan-gold nanoparticle nanocomposite films

Xiu-Xiu Dong[a], **Jin-Yi Yang**[a], **Lin Luo**[a], **Yi-Feng Zhang**[a], **Chuanbin Mao**[b,c,*], **Yuan-Ming Sun**[a], **Hong-Tao Lei**[a], **Yu-Dong Shen**[a], **Ross C. Beier**[d], and **Zhen-Lin Xu**[a,**]

[a]Guangdong Provincial Key Laboratory of Food Quality and Safety, South China Agricultural University, Guangzhou 510642, China

[b]Department of Chemistry and Biochemistry, University of Oklahoma, 101 Stephenson Parkway, Norman, OK 73019, USA

[c]School of Materials Science and Engineering, Zhejiang University, Hangzhou, Zhejiang 310027, China

[d]US Department of Agriculture, Agricultural Research Service, Southern Plains Agricultural Research Center, Food and Feed Safety Research Unit, College Station, TX 77845, USA

Abstract

Histamine (HA) is a biogenic amine that can accumulate to high concentration levels in food as a result of microbial activity and can cause toxic effects in consumers. In this work, a portable electrochemical immunosensor capable of detecting HA with high sensitivity and selectivity was developed. Prussian blue-chitosan-gold nanoparticle (PB-CS-AuNP) nanocomposite films with excellent biocompatibility were synthesized and characterized by scanning electron microscopy and energy dispersive X-ray analysis. The PB-CS-AuNP were coated onto a screen-printed electrode by one-step electrodeposition and used to conjugate the HA ovalbumin conjugate (HA-Ag). HA was determined by a competition between the coating HA-Ag and the HRP labeled HA antibody (HRP-HA-Ab). After careful optimization of assay conditions and Box-Behnken analysis, the developed immunosensor showed a linear range from 0.01 to 100 μg/mL for HA in fish samples. The average recoveries from spiked samples ranged from 97.25% to 105%. The biosensor also showed good specificity, reproducibility, and stability, indicating its potential application in monitoring HA in a simple and low cost manner.

Keywords

Histamine; Immunosensor; Prussian blue-chitosan-gold nanoparticles; Food analysis

[*]Corresponding author at: Department of Chemistry and Biochemistry, University of Oklahoma, 101 Stephenson Parkway, Norman, OK 73019-3051, USA. [**]Correspondence to: Guangdong Provincial Key Laboratory of Food Quality and Safety, South China Agricultural University, No. 483, Wushan Street, Guangzhou 510642, China. cbmao@ou.edu (C. Mao), jallent@163.com (Z.-L. Xu).

1. Introduction

Histamine (HA), 4-(2-aminoethyl)-1H-imidazole, is one of the most important biogenic amines in relation to allergies and food poisonings. It is released from mast cells, basophils, and a vast array of other cells including normal and malignant lymphocytes (Jiang et al., 2015; An et al., 2016). HA is related to the spoiling of food (including meat, eggs, chocolate, cheese, and wine) and is the leading cause of foodborne illness associated with the consumption of fish containing high levels of HA (Stratton et al., 1991). Therefore, HA is used as an indicator of food preservation and quality assurance in consumable products (Martuscelli et al., 2013; Pérez et al., 2013).

Various analytical methods have been developed to separate and measure the content of HA. The most common analysis techniques include the fluorometric method (Ough, 1971), high-performance liquid chromatography (HPLC) (Romero-González et al., 2012; Chen et al., 2016), and gas chromatography (GC) (Hwang et al., 2003). The instrumental methods such as HPLC and GC are laborious and expensive, while the fluorometric method does not meet the requirements of sensitivity for quantitative determination. Antibody based immunoassays, such as the enzyme-linked immunosorbent assay (ELISA), have been proven to be rapid, sensitive, and low-cost screening tools for chemical residue analysis. Several ELISAs have been developed for HA (usually specific for a derivative of HA) in blood or food samples (Rauch et al., 1992; Serrar et al., 1995). We have produced a monoclonal antibody against a novel HA derivative and developed an ELISA method for the analysis of HA in food samples (Luo et al., 2014).

As an alternative to traditional ELISAs, biosensors can be attractive analytical tools offering fast and reduced analysis time methods, while still demonstrating adequate selectivity and sensitivity. Several electrochemical biosensors (Pérez et al., 2013; Dai et al., 2014; Jiang et al., 2015; Veseli et al., 2016) have been reported for the determination of HA. Most of these biosensors are based on enzymes or nanozymes (such as diamine oxidase). However, the specificity cannot be guaranteed with these biosensors since the enzyme can simultaneously catalyze HA and its analogues. Immunosensors have superior characteristics due to the high sensitivity and good specificity of antibody-antigen interactions (J. Zhang et al., 2016; Y. Zhang et al., 2016; Z. Zhang et al., 2016).

Nanomaterials are often used to improve the sensitivity of biosensors by amplifying their conductivity, catalytic activity, and biocompatibility signals (Ma et al., 2013; Song et al., 2016). Prussian blue (PB) exhibits good electrocatalytic activity (W. Wang et al., 2014) and PB-based nanocomposites are primarily used for the immobilization of enzymes to fabricate an enzymatic biosensor (Zhang et al., 2011; Wang et al., 2012; B. Wang et al., 2014). Gold nanoparticles (AuNPs) can better facilitate electron transfer and produce signal amplification for electrochemical detection as a sensor platform (Miao et al., 2016). However, the unique structure and remarkable advantages of using PB-AuNP for immunosensors and biosensing applications have not yet been recognized.

In this work, a sensitive and selective electrochemical immunosensor was constructed to detect HA by assembling a PB-CS-AuNP nanocomposite film on a screen-printed carbon

electrode (SPCE) to capture HA-Ag and HRP-HA-Ab as the signal label. After careful study of the assay conditions, the constructed immunosensor then had the appropriate sensitivity and selectivity to determine HA in fish samples by the catalytic reaction between HRP and H_2O_2, using hydroquinone (HQ) as an electron mediator.

2. Materials and methods

2.1. Reagents

HA dihydrochloride, L-histidine, tryptamine hydrochloride, tyramine hydrochloride, phenethylamine hydrochloride, cadaverine hydrochloride, methyl 4-(chlorocarbonyl)benzoate, *p*-nitrobenzoic acid, and triethylamine were obtained from Aladdin Chemical Technology Co., Ltd. (Shanghai, China). Gold (III) chloride tetrahydrate ($AuCl_3{\cdot}HCl{\cdot}4H_2O$, 99.9%) was obtained from the Shanghai Chemical Reagent Co., Ltd. (Shanghai, China) HRP was obtained from Roche (Shanghai, China). HA-antibody (HA-Ab) and HA-antigen (HA-Ag) were prepared in our laboratory. All other chemicals were of analytical grade or better and used as received without further purification.

Buffers and solutions used in this work can be found in the Supporting materials.

2.2. Apparatus

Electrochemical measurements were performed on a CHI660D electrochemical work station (CH Instruments, Shanghai Chenhua Instrument Corporation, Shanghai, China) with a portable commercial screen-printed carbon electrode (SPCE, Zensor R & D, Taiwan), which consisted of a carbon working electrode (3 mm diameter), a carbon auxiliary electrode and an Ag/AgCl reference electrode. Scanning electron microscopy (SEM) was carried out on a field emission scanning electron microscope, JSM-6700F (JEOL USA, Inc., Peabody, MA, USA). The UV–vis spectra were performed using a UV2550 Spectrometer (Shimadzu, Japan).

2.3. Preparation of HRP-HA-Ab label

The signal tag (HRP) was conjugated to the HA antibody to form the HRP-HA-Ab as described by Tsang et al. (1995), with modifications. The details of the conjugation procedure can be found in the Supporting materials.

2.4. Construction of the HA immunosensor

Scheme 1 illustrates the stepwise fabrication of the immunosensor. The PB-CS-AuNP nanocomposite film was electrodeposited on the SPCE. Then a solution of HA-Ag was coated on the working surface of the SPCE. Subsequently, the blocking solution was coated on the electrode surface to block the possible remaining active sites to avoid nonspecific binding. Finally, the immunosensor was thoroughly washed with 0.01 M PBS and stored at 4 °C until used. For detection the modified immunosensor was immersed in a 1/15 M PBS solution containing 1 mM HQ and 1.44 mM H_2O_2. The change in the electrochemical cathodic current before and after addition of H_2O_2 was used as the signal response. The detailed steps of immunosensor construction as well as the diagram of the portable sensor and electric circuit can be found in the Supporting materials (Figs. S1 and S2).

2.5. Statistical design and analysis

To better understand the effect of assay conditions on immunosensor performance, the single-factor data were subjected to analysis via the Box-Behnken design with a total of three factors, one at each of the three levels. It includes 14 experimental points per test. The complete experiment was repeated three times to statistically develop the second order polynomial model shown in Eq. (1).

$$Y=\beta 0+\sum_{i=1}^{3}\beta \mathrm{i}Xi+\sum_{i=1}^{3}\beta \mathrm{ii}XiXi+\sum_{i=1}^{3}\sum_{j=i+1}^{3}\beta \mathrm{ij}XiYj \quad (1)$$

Where Y represents the response variable; β_0 is the interception coefficient; β_i, coefficient of the linear effect; β_{ii}, coefficient of quadratic effect; β_{ij}, the coefficient of interaction effect; and X_i and X_j are independent variables. Experiments were designed and analyzed in Design-Expert version 10 software (Stat-Ease, Inc., Minneapolis, MN, USA). Each independent variable was coded at three levels, −1, 0 and 1, corresponding to a low un-coded level, middle and high levels, respectively.

2.6. Preparation of fish samples

The fish samples were prepared as described by Luo et al. (2014). Fish samples were homogenized and spiked with the HA standard, and then submitted for extraction and derivatization. A dilution of 1:100 was used with all samples to eliminate the matrix effects, and then the samples were submitted for immunosensor analysis.

3. Results and discussion

3.1. Characterization of PB-CS-AuNP and electrochemical behavior of the HA immunosensor

SEM was used to characterize the morphology of the electrodeposited PB-CS-AuNP nanocomposite film on the SPCE. As shown in Fig. 1A, the nanocomposite film resembles a bunch of grapes, with a high surface area, and is homogeneously spread out on the surface of the electrode. PB-CS and AuNPs-CS were equally deposited on the electrodes. In Fig. 1B and C shows the PB-CS has some heterogeneous bulges and scattered AuNPs are spread on the AuNPs-CS film. Compared to PB-CS and AuNPs-CS films, PB-CS-AuNP were clearly surrounded by a blurry film with a cluster, which was attributed to the adhesion of CS on PB wrapped with AuNPs. This phenomenon may be exhibited by energy dispersive X-ray analysis (EDX, Fig. 1D) and is consistent with an earlier research report (B. Wang et al., 2014).

The CVs of the different modified electrodes in the 0.1 mol/L KCl solution containing 1 mmol/L $[Fe(CN)_6]^{3-/4-}$ at a scan rate of 50 mV/s are shown in Fig. 1E. Compared to the bare SPCE, the oxidation/reduction currents are all enhanced on the AuNPs-CS, PB-CS and PB-CS-AuNP modified SPCE. The sequence for the values of electroactive surface areas (A) for the different electrodes is the following: PB-CS-AuNPs/SPCE > PB-CS/SPCE >

AuNPs-CS/SPCE > SPCE (Zhou et al., 2008). It is clear that the PB-CS-AuNP film modified SPCE has more favorable electron transfer kinetics.

Traditionally, the immunosensor was developed using a two-step method, the first antibody would capture the coating antigen followed by the addition of an enzyme labeled second antibody, which is a common commercial product (Zang et al., 2013; He et al., 2015). This method requires two incubation and washing steps. To save assay time and simplify the procedure, we directly labeled HRP to the HA antibody to form a bi-functional reagent (HRP-HA-Ab). As shown in Fig. 1F, the synthesized HRP-HA-Ab demonstrated qualitative differences between HRP and the Ab in the UV–vis spectra, suggesting a successful conjugation of HRP to the HA antibody.

3.2. Optimization of analytical conditions for the immunosensor

Several analytical conditions were optimized, such as the dilution ratio of HRP-HA-Ab, the dilution ratio of HA-Ag, the incubation time of HRP-HA-Ab and HA-Ag, and the concentration of H_2O_2. A single-factor test was applied and the results are shown in the Supporting materials (Fig. S3). When testing the dilution needed for HRP-HA-Ab, the signal response exhibited a continuous increase until the dilution ratio reached 1:100, and the response value showed a slight decrease when the dilution ratio was further reduced. Therefore, the dilution ratio of 1:100 was chosen for subsequent experiments. Similarly, a dilution ratio of 1:200 for HA-Ag, and a 2 h incubation time and 1.44 mM for the H_2O_2 concentration were chosen for the optimal assay conditions.

To further optimize the assay conditions, a Box-Behnken analysis based on the results of a single-factor test was applied. The proposed values vs. actual values (Table S1), and model analysis (Table S2) suggested the suitability of the developed model for the immunosensor signal response. The contour plots resulting from the Box-Behnken analysis can also be found in the Supporting materials (Fig. S4). The data shows that the dilution ratio of 1:166 for HA-Ag, the dilution ratio of 1:62 for HRP-HA-Ab, and the incubation time of 2.2 h would produce the highest signal response for the immunosensor (12.28 μA) with a relative standard deviation (RSD) of 0.036. It should be noted that these optimal values are important references for the experiment. Since the optimal conditions of Box-Behnken analysis are very similar to the single-factor test, the conditions used for the following study include the dilution ratio of 1:200 for HA-Ag, the dilution ratio of 1:100 for HRP-HA-Ab, and the incubation time of 2 h.

3.3. HA immunosensor performance

Under optimal conditions, the constructed immunosensor based on the PB-CS-AuNP platform and HRP-HA-Ab label was applied to detect different concentrations of HA (0.01, 0.05, 0.1, 0.5, 1, 5, 50 and 100 ng/mL) (Fig. 2). In a typical competitive immunoassay, a standard HA solution was added at equal volumes into the incubation solution containing 0.1 mg/mL HRP-HA-Ab. Then 6 μL of the mixture was immediately incubated on the immunosensor surface. HA in the incubation solution was then free to compete with the immobilized HA-Ag on the immunosensor surface to combine with the limited binding sites of HRP-HA-Ab and form an immunocomplex. A low concentration of HA resulted in a

larger current change due to the formation of more immunocomplex on the sensor surface. Alternatively, a high concentration of HA resulted in little current change, and ΔI gradually decreased with the increase in HA concentrations (Fig. 2B). Furthermore, a linear response was discovered between ΔI and the logarithm of the HA concentration in the range of 0.01–100 ng/mL represented by $\Delta I\ (\mu A) = (6.48 \pm 0.1) - (2.5 \pm 0.08) \times \lg C_{HA}\ (ng/mL)$ with a correlation coefficient of 99.3%, where ΔI is the current change and C is the HA concentration. In addition, according to the equation (Analytical Chemistry Division, 1978): $x_L = x_{b1} + 3s_{b1}$, where x_L is the detection limit, x_{b1} is the mean signal of the blank measurement, s_{b1} is the standard deviation of the blank measurement, and a value of 3 is chosen for the equation constant. For practical purposes this corresponds to about a 90% confidence level, while the detection limit can be calculated at 1.25 pg/mL. Finally, we compared the analytical performance of the constructed electrode with some recent references (Supporting materials, Table S3). The comparison revealed that the developed sensor has a wider linear range, lower detection limit and higher sensitivity than other published sensors.

3.4. Specificity, reproducibility and stability of the immunosensor

To evaluate the selectivity range of the immunosensor for detection of HA, the cross-reactivity (CR) against a range of analogues compared to HA, such as L-histidine, trytamine, tryamine, phenethylamine and cadaverine were examined under the same experimental conditions. As shown in Table S4 (Supporting materials), The CRs were lower than 0.1% for all the analogues tested, suggesting that these analogues should not interfere with HA detection. Although, these structural analogues also belong to the same class of biogenic amines, and some of them have a similar chemical structure as HA, this electrochemical immunosensor demonstrated a high specificity for the detection of HA. The superior specificity of the developed immunosensor is partially determined by the characteristics of the prepared antibody.

The reproducibility of the immunosensor is an important parameter for assessing its practical application. In this study, reproducibility was confirmed by six measurements at every HA concentration, which resulted in the relative standard deviations of 2.5%, 1.85% and 3.61% at HA concentrations of 0.4, 4 and 40 ng/mL, respectively.

The stability of the biosensor was also explored by periodically evaluating its catalytic current response. When the biosensor was not in use, it was stored in a refrigerator at 4 °C. After 2 weeks, the catalytic current of the immunosensor was about 84.3% of its original value (which decreased by about 15.7%), indicating retention of the specific binding ability of the antigen was acceptable.

3.5. Detection of HA in spiked fish samples

Fish samples were analyzed after spiking with HA concentrations at 0.4, 4, and 40 ng/mL (n = 3). Average recoveries were observed from 97.25% to 105% with the coefficient of variance (CV) ranging from 0.91% to 2.07% (Table S5). These results demonstrated that the matrix effect of the samples was negligible using the described sample preparation method.

To confirm the reliability of the constructed immunosensor, portions of the spiked fish samples were also subjected to HA analysis by LC−MS/MS. The results of the immunosensor were in good agreement with those of LC−MS/MS (Table S5), revealing good reliability and accuracy for the immunosensor.

4. Conclusion

In summary, we have developed a PB-CS-AuNP nanocomposite film and HRP-HA-Ab label based platform that can be used to develop a super-sensitive immunosensor for the determination of HA in fish samples. The immunosensor can determine HA in the range of 0.01–100 μg/mL in fish samples, with only a simple sample pretreatment. The developed electrochemical immunosensor exhibited good specificity, acceptable stability and reproducibility, which was necessary for screening HA residues in fish samples. The immunosensor platform also should be useful for developing super-sensitive analytical methods for other molecules.

Supplementary Material

Refer to Web version on PubMed Central for supplementary material.

Acknowledgments

This work was supported by The National Key Research and Development Program of China (2016YFD0401204), the Innovation Team Foundation of the Department of Agriculture of Guangdong Province (2016LM2152), the Guangdong Natural Science Funds for Distinguished Young Scholar (2014A030306026), the Excellent Young Teachers Program for Higher Education of Guangdong Province (Y920/4026), and the Guangdong Special Support Program (2014TQ01N109). CM would also like to thank the financial support from the National Institutes of Health (CA195607 and EB021339) and Department of Defense Office of Congressionally Directed Medical Research Programs (W81XWH-15-1-0180).

Appendix A. Supplementary material

Supplementary data associated with this article can be found in the online version at http://dx.doi.org/10.1016/j.bios.2017.07.014.

References

Analytical Chemistry Division. Spectrochim Acta. 1978; B 33:241–245.

An D, Chen Z, Zheng Z, Chen J, Wang S, Su W. Food Chem. 2016; 194:966–971. [PubMed: 26471641]

Chen R, Deng Y, Yang L, Wang J, Xu F. J Chromatogr Sci. 2016; 54:547–553. [PubMed: 26688564]

Dai J, Zhang Y, Pan M, Kong L, Wang S. J Agric Food Chem. 2014; 62:5269–5274. [PubMed: 24823260]

He Z, Zang S, Liu Y, He Y, Lei H. Biosens Bioelectron. 2015; 73:85–92. [PubMed: 26047998]

Hwang BS, Wang JT, Choong YM. Food Chem. 2003; 82:329–334.

Jiang S, Peng Y, Ning B, Bai J, Liu Y, Zhang N, Gao Z. Sens Actuators B-Chem. 2015; 221:15–21.

Luo L, Xu ZL, Yang JY, Xiao ZL, Li YJ, Beier RC, Sun YM, Lei HT, Wang H, Shen YD. J Agric Food Chem. 2014; 62:12299–12308. [PubMed: 25417820]

Ma J, Cai P, Qi W, Kong D, Wang H. Colloid Surf. 2013; A 426:6–11.

Martuscelli M, Arfelli G, Manetta AC, Suzzi G. Food Chem. 2013; 140:590–597. [PubMed: 23601412]

Miao X, Li Z, Zhu A, Feng Z, Tian J, Peng X. Biosens Bioelectron. 2016; 83:39–44. [PubMed: 27101533]

Ough CS. J Agric Food Chem. 1971; 19:241–244. [PubMed: 5546152]

Pérez S, Bartrolí J, Fàbregas E. Food Chem. 2013; 141:4066–4072. [PubMed: 23993586]

Rauch P, Rychetsky P, Hochel I, Bilek R, Guesdon JL. Food Agric Immunol. 1992; 4:67–72.

Romero-González R, Alarcón-Flores MI, Vidal JLM, Frenich AG. J Agric Food Chem. 2012; 60:5324–5329. [PubMed: 22559197]

Serrar D, Brebant R, Bruneau S, Denoyel GA. Food Chem. 1995; 54:85–91.

Song Y, Luo Y, Zhu C, Li H, Du D, Lin Y. Biosens Bioelectron. 2016; 76:195–212. [PubMed: 26187396]

Stratton JE, Hutkins RW, Taylor SL. J Food Prot. 1991; 54:460–470.

Tsang VCW, Greene RM, Pilcher JB. J Immunoass. 1995; 16:395–418.

Veseli A, Vasjari M, Arbneshi T, Hajrizi A, Švorc Ľ, Samphao A, Kalcher K. Sens Actuators B-Chem. 2016; 228:774–781.

Wang B, Ji X, Zhao H, Wang N, Li X, Ni R, Liu Y. Biosens Bioelectron. 2014a; 55:113–119. [PubMed: 24368228]

Wang W, Qin C, Xie Q, Qin X, Chao L, Huang Y, Dai M, Chen C, Huang J, Hu J. Analyst. 2014b; 139:2904–2911. [PubMed: 24761432]

Wang L, Ye Y, Zhu H, Song Y, He S, Xu F, Hou H. Nanotechnology. 2012; 23(45):455502. (10pp.). [PubMed: 23090569]

Zang S, Liu Y, Lin M, Kang J, Sun Y, Lei H. Electrochim Acta. 2013; 90:246–253.

Zhang Z, Duan F, He L, Peng D, Yan F, Wang M, Zong W, Jia C. Microchim Acta. 2016c; 183:1089–1097.

Zhang Y, Li J, Wang Z, Ma H, Wu D, Cheng Q, Wei Q. Sci Rep. 2016b; 6(23391) (8pp.).

Zhang J, Sun Y, Dong H, Zhang X, Wang W. Sens Actuators B-Chem. 2016a; 233:624–632.

Zhang M, Yuan R, Chai Y, Li W, Zhong H, Wang C. Bioprocess Biosyst Eng. 2011; 34:1143–1150. [PubMed: 21720965]

Zhou M, Guo J, Guo LP, Bai J. Anal Chem. 2008; 80:4642–4650. [PubMed: 18476717]

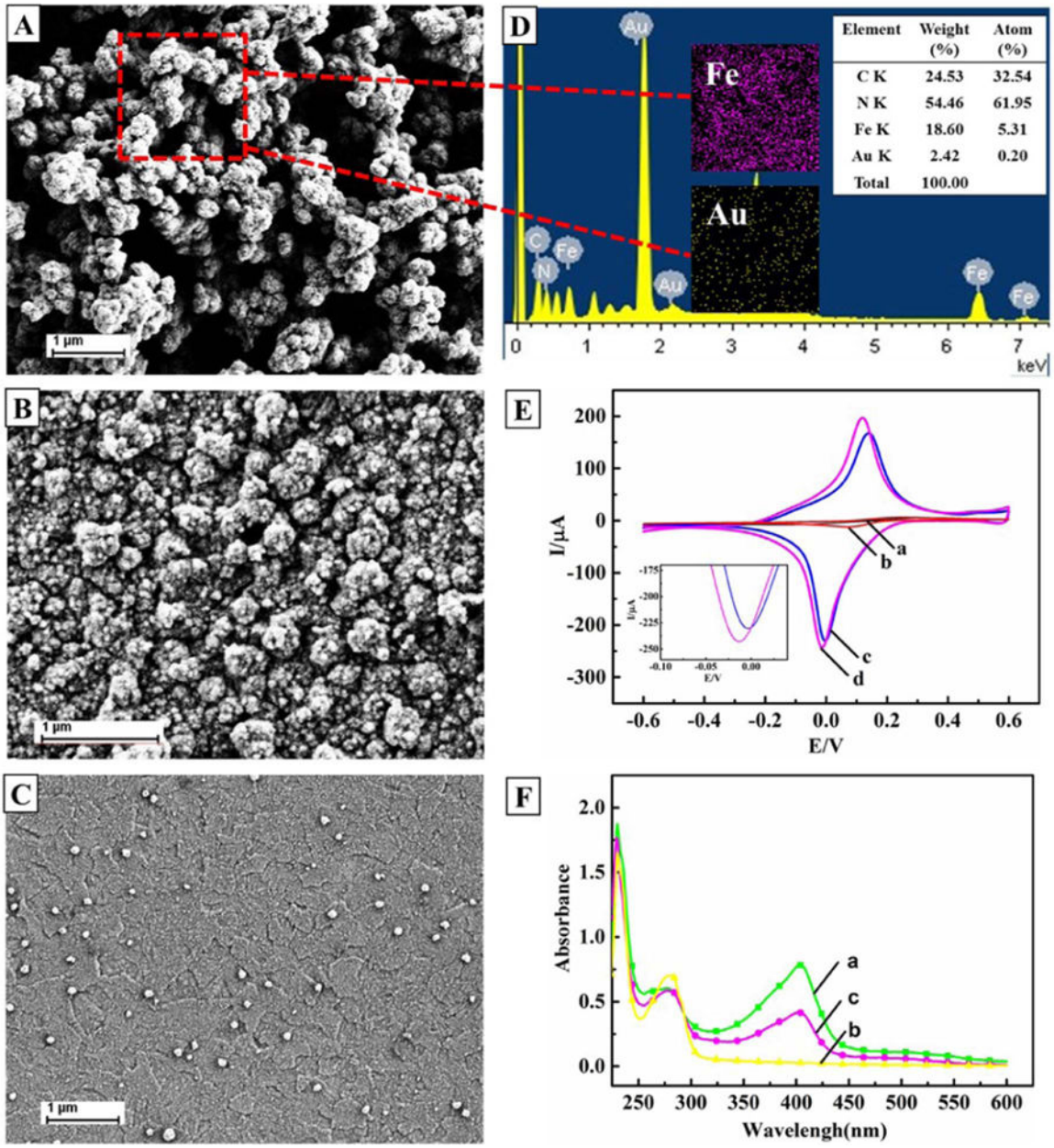

Fig. 1.

A) Characterization of PB-CS-AuNP; B) PB-CS; C) AuNPs-CS; D) nanocomposite films by SEM imaging, and EDS analysis of PB-CS-AuNP; E) the two inset illustrations are the elemental mappings of Fe (pink) and Au (yellow); and F) Cyclic voltammograms at a scan rate of 50 mV/s. (a), (b), (c) and (d) are from a bare SPCE, AuNPs-CS/SPCE, PB-CS/SPCE and PB-CS-AuNPs/SPCE, respectively, in 0.1 mol/L KCl solution containing 1 mmol/L $[Fe(CN)_6]^{3-/4-}$; These curves are the UV–vis spectra of: (a) HRP, (b) HA-Ab and (c) HRP-HA-Ab.

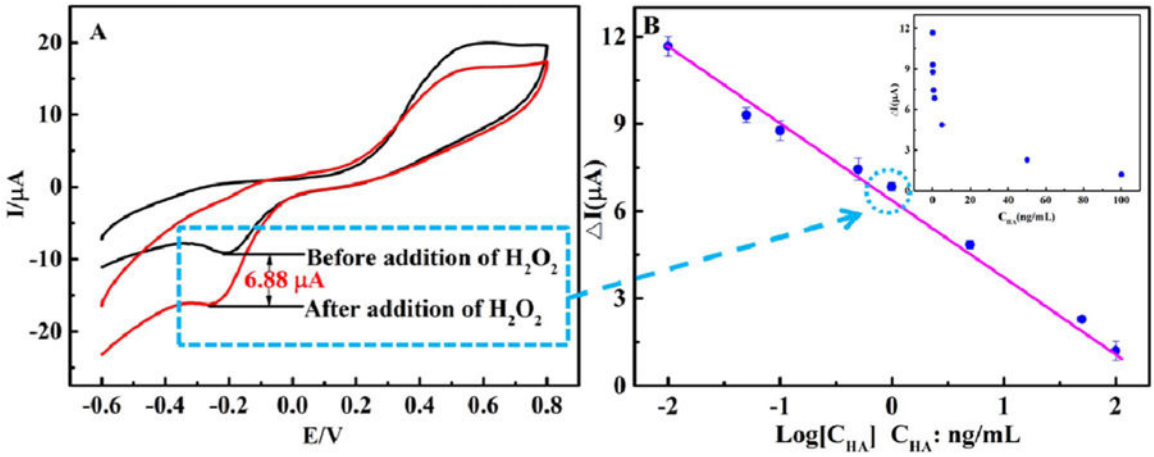

Fig. 2.

A) Cyclic voltammograms; and B) calibration curve of the immunosensor and the relationship (inset in (B)) between the concentration of HA (C_{HA}) and the current response (ΔI) of the standard solution.

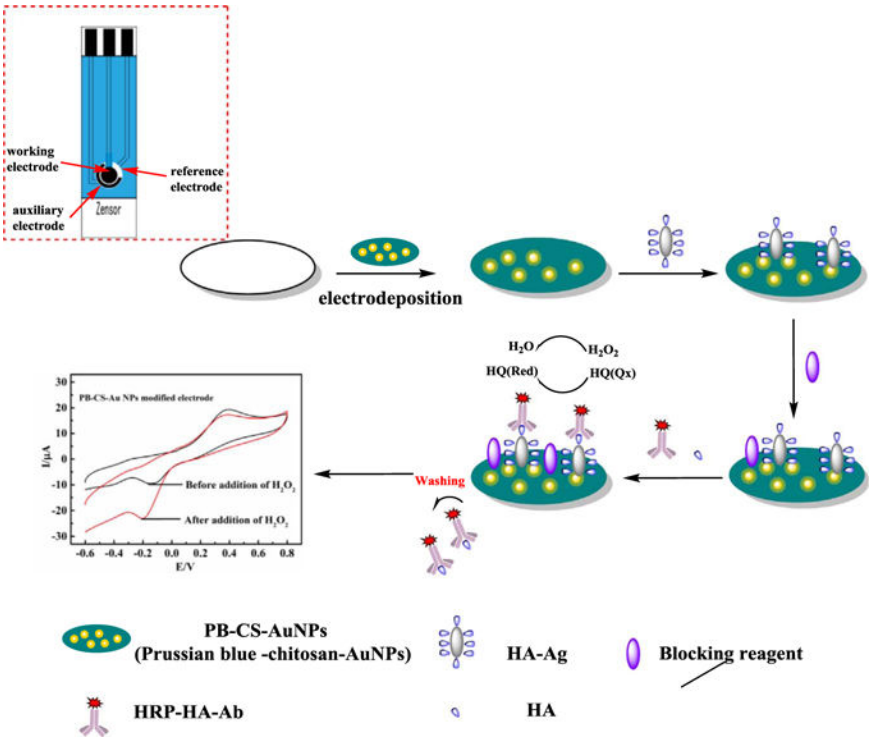

Scheme 1.

Schematic representation of the HA immunosensor with a one-step electrodeposition of PB-CS-AuNP nanocomposite film using HRP-HA-Ab as the label with the aid of the electron mediator (HQ) and H_2O_2.